

Photocatalytic degradation of turquoise blue textile dye using silver nanoparticles prepared from aqueous Kecemcem (*Spondias pinnata*) leaf extract

Ngurah Wijaya Putra^{1*}, I Wayan Budiarsa Suyasa², I Wayan Suarna²,
Anak Agung Sagung Alit Sukmaningsih³, I Dewa Ketut Sastrawidana⁴

¹ Doctoral Program of Environmental Science Student, Udayana University, Denpasar, Bali, Indonesia

² Environmental Science Postgraduated Program, Udayana University, Denpasar, Bali, Indonesia

³ Biology Study Program of Mathematics and Natural Sciences Faculty, Udayana University, Jimbaran, Bali, Indonesia

⁴ Department of Chemistry, Faculty of Mathematics and Natural Sciences, Universitas Pendidikan Ganesha, Singaraja 81117 Bali, Indonesia

* Corresponding author's e-mail: ngr.wijayaputra@gmail.com

ABSTRACT

Silver nanoparticles (AgNPs) were generated utilizing Kecemcem (*Spondias pinnata*) leaf extract, and their efficacy in the photocatalysis of turquoise blue textile dye was assessed through a batch method. The produced AgNPs were characterized by identify characteristic absorption band using UV-visible spectroscopy. the functional groups using FTIR, the crystalline phase, structure, and size through XRD. The photoactive degradation of dye using AgNPs was examined under 50-watt UV irradiation at different initial pH mediums, AgNPs-to-dye volume ratios, dye concentrations, and lengths of exposure time. The AgNP creation is suggested by a color change from yellow to reddish brown and is supported by the UV-visible spectrum, which generally appears 420 nm. The functional groups contained in AgNPs were identified from FTIR analysis in the range 1066–3329 cm^{-1} . The signal at 3329.14 cm^{-1} is assigned to OH stretching, while the peaks at 1631.7 cm^{-1} and 1386 cm^{-1} are compatible with C=C and C-C stretching of alkenes, as well as C-H stretching of amide bonds, confirming the presence of protein. Additionally, the signal at 1066.64 cm^{-1} indicates to C-O stretching of carbonyl functional group. Based on XRD data, it was confirmed that the crystalline phase of AgNPs was 54.35% with a crystal size of 22 nm, and the peaks observed at 2θ values of around 38.21°, 46.45°, 66.65°, and 77.55° showed the 111, 200, 220, and 311 planes of the cubic face-centered structure. The photocatalytic degradation efficiency of 125 mg/L turquoise blue textile dye of 94.57% was achieved at operational conditions of pH 5, the addition of 6 mL AgNPs per 100 mL dye, and irradiation with a 50-watt UV lamp for 150 mins. These results imply that silver nanoparticles prepared using bioreductants contained in Kecemcem leaf extract are very promising for treating organic contaminants found in textile wastewater.

Keywords: Kecemcem leaf extract, silver nanoparticles, photocatalytic degradation, turquoise blue dye.

INTRODUCTION

Textile industries generate wastewater that contains various contaminants such as dyes and heavy metals, which pose a serious environmental risk when directly discharged without proper treatment. Textile wastewater is highly toxic and contains suspended solids, chemical oxygen demand, high dye concentrations, and

various chemicals as well as heavy metals [Kumar, 2017; Tabish et al., 2024]. The examination of several physical and chemical parameters in textile wastewater conducted by Dhameliya and Ambasana (2023) found that textile wastewater from the sequential process stage, including bleaching, mercerization, printing, and washing, had a pH value of 13.1, BOD of 1840 mg/L, COD of 4449 mg/L, TSS of 1189 mg/L, and TDS of

21989 mg/L. These parameters value are over the threshold of quality standards required in the Republic Nation of Indonesian regulations regarding textile wastewater quality standards, where the permitted pH value is in the range of 6–9, as well as the maximum value of COD, BOD, TSS, and heavy metal values are 150, 60, 50, and 1.0 mg/L, respectively. In addition, water bodies containing dyes can inhibit the penetration of sunlight into the water, which results in an oxygen decrease, thus endangering the aquatic life system. The majority of dyes applied in the dyeing process are from the azo dye family.

Azo dyes are the chemicals containing the functional group $R-N=N-R$ within their molecular structure. This azo group of dyes is the most popular used in textile dyeing, printing, food and cosmetic manufacture, and it is estimated that more than 60% of the dyes used are of this dye group [El-Sayed et al., 2024]. In general, azo dyes are inherently resistant to natural decomposition due to their robust chemical structure, resulting in detrimental effects on aquatic ecosystems when the textile wastewater effluent is discharged into water bodies. Most azo dyes exhibit carcinogenic, mutagenic activities and allergic reactions [Strebel et al., 2024].

Different treatment methods, including biological, physical, and chemical, have been developed to degrade textile dyes and real wastewater. Biological approaches using anaerobic and aerobic bacteria (Fajri et al., 2024), Khamir [Sukarta et al., 2021], and wood-degrading fungi [Sudiana et al., 2022] are able to degrade dyes with high removal efficiency, but they have several limitations, especially requiring long operating times and being very sensitive to experimental conditions. As a consequence, the biological treatment is less successful when applied to wastewater containing high dye concentrations. The physical treatment methods include adsorption by activated coconut leaf stalk [Sudiana et al., 2022], coagulation and flocculation [Bressan et al., 2024], and photocatalysis using hydroxyapatite/titania composite [Sukarta and Sastrawidana, 2024]. Degradation of pollutants through photocatalytic techniques has several superior treatments over other treatment methods, such as their simplicity of operation, relatively low operating cost, and high removal efficiency for pollutants [Saeed et al., 2021; Zayed et al., 2022]. In photocatalysis, when light with energy equal to or more than the semiconductor band gap are absorbed by a semiconductor, the photocatalytic destruction of dyes begins. Superoxide radicals

($\bullet O_2^{2-}$) and hydroxyl radicals ($\bullet OH$) are produced when electrons are moved from the valence band to the conduction band, forming the electron (e^-) and hole (h^+) bands. Both these radicals effectively break down the dyes through redox reactions [Pingmuang et al., 2017; Nazri and Sapawe, 2020]. Several heterogeneous photocatalysts are used for the dye removal, such as ZnO, TiO_2 , CdS, and nanoparticles of metal such as gold, silver and zinc [Paul et al., 2020].

Silver nanoparticles (AgNPs) are nanomaterials composed of silver elements. This AgNPs can be used for photocatalytic decomposition of contaminants from wastewater due to their exclusive characteristics, such as larger surface area, smaller size, high thermal stability, antibacterial properties, and high catalytic activity [Jaast and Grewal, 2021]. Besides that, the AgNPs have also been utilized in biomedical and biological applications, including medical device coatings, anti-cancer therapy, bone healing, agents of anti-diabetic, drug delivery, and antimicrobials [Xu et al., 2020; Meher et al., 2024], agricultural, such as to enhance seed germination, plant growth, nanopesticides, and fertilizer [Khan et al., 2023], and applications for energy storage, like electrochemical sensors and supercapacitors [Salve et al., 2020].

The AgNPs can be created by applying a diversity of techniques, like physical, chemical, and biological methods. However, biological techniques are preferred because they are scalable, economical, and ecologically benign [Parvathiraja et al., 2021]. In addition, the physical and chemical methods frequently use the harmful chemicals that may endanger the environment. To minimize environmental risks, recently the preparation of AgNPs using plant extracts has received increasing consideration due to its environmentally friendly properties [Verma et al., 2016]. The plants containing reductant agents such as flavonoids, alkaloids, terpenoids, saponins, and tannins are potentially used in the synthesis of AgNPs. Some plant extracts that have been successfully used to synthesize AgNPs include horseradish, neem, fenugreek, bitter apple, raphanus sativus, beta vulgaris, and *Ocimum basilicum* [Velusamy et al., 2015; Garciduenas-Pina et al., 2023; Abada et al., 2024].

In Bali of Indonesia, Kecemcem leaves are widely consumed fresh as salad or made into a traditional herbal drink known as 'loloh.' In addition, this plant is believed to be part of traditional Balinese ethnobotany for the treatment of diabetes, gastric ulcers, and urolithiasis [Sujarwo

et al., 2015]. Phytochemical examination of Kecemcem leaf extract was found to contain flavonoids, terpenoids, tannins, phenols, and alkaloids [Cahyawati et al., 2019]. By considering its abundant availability, ease of obtaining, and the phytochemicals in the Kecemcem leaf, this biomedical plant extract is a possible option for use as a bioreductant in the preparation of AgNPs. The aim of this work was to investigate the ability of AgNPs produced from the aqueous extract of Kecemcem leaf to breakdown turquoise blue textile dye. The produced AgNPs were characterized by their wavelength using a UV-Vis spectrophotometer, functional groups using FTIR, crystal phase using XRD, and surface morphology using SEM-EDX. Furthermore, the AgNPs were analyzed for their capability to degrade anionic turquoise blue dye photocatalytically irradiated by a 50-watt UV lamp. The operational parameters studied included the impact of pH, AgNP to dye volume ratio, concentration of dye, and exposure time on the efficiency of photocatalytic degradation.

MATERIALS AND METHODS

Materials

The primary compounds utilized in this study, such as AgNO_3 , NH_4OH , H_2SO_4 , HCl , FeCl_3 , and chloroform, are of analytical grade purity. The Kecemcem leaf (*Spondias pinnata*) was obtained from Bangli regency, while turquoise blue dye was obtained from Sigma-Aldrich. The dye molecular configuration is displayed in Figure 1.

Preparation of aqueous kecemcem leaf extract

Kecemcem leaves have been cleaned with distilled water to eliminate their contaminants and then left in a room without light for seven days to dry. Dried Kecemcem leaves are crushed into powder with a blender machine and then sieved

with a 50-mesh sieve size. Twenty grams of Kecemcem leaf powder was put in a 250-mL beaker glass consisting of 100 mL of water and heated at 60 °C for 15 minutes. Following cooling, the mixture was filtered using size 42 Whatman filter paper. The aqueous Kecemcem leaf extract was evaporated using a vacuum evaporator to obtain concentrated Kecemcem leaf extract.

Qualitative identification of phytochemicals from kecemcem leaf extract

Bioreductants such as alkaloids, flavonoids, terpenoids, steroids, tannins, and saponins contained in the water extract used for the preparation of AgNPs were identified qualitatively using certain reagents. The alkaloids test is conducted using Dragendroff, Wagner, and Mayer reagents; the flavonoid test is using Shinod's test; terpenoids and steroids are tested through Liebermann-Buchard reagents; the test for saponins is using the foam test; and the test for tannins is with ferric chloride solution. They are identified based on the characteristic color change and the precipitate formed.

The AgNPs synthesis

The AgNPs were prepared using 1 mM silver nitrate to aqueous extract of Kecemcel leaf volume ratio of 0.5. An amount of 50 mL of 1 mM AgNO_3 solution was transferred in a glass beaker containing 100 mL of aqueous Kecemcem leaf extract, and the concoction was heated at 60 °C for 15 mins. The change in color of the mixture from yellow to reddish brown indicates that AgNPs have been formed.

Characterization of AgNPs

The characteristics of the synthesized AgNPs include determining the maximum wavelength using a Shimadzu UV-Vis spectrophotometer, identifying functional groups using FTIR, and analyzing the crystalline phase and particle size using XRD.

Photocatalytic degradation studies

The breakdown of turquoise blue dye solution by photocatalysis with AgNPs was conducted in a batch system. A total of 10 mL of AgNPs was transferred to the photocatalytic reactor containing 100 mL of 25 mg/L turquoise blue dye solution and then irradiated with 50 watts of UV light for 180 minutes. The various operating variables are examined, including the impact of AgNPs to dye volume ratio,

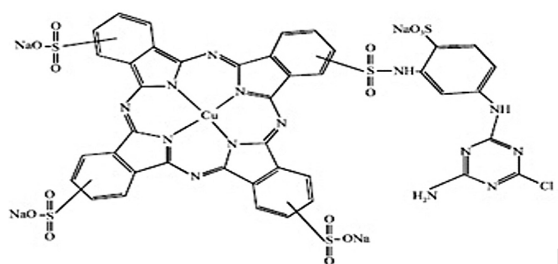


Figure 1. Molecular structure of the turquoise blue dye

initial pH and concentration of dye solution, and irradiation duration time. The absorbance of dye before and after treatment was determined through a UV-Vis spectrophotometer at 615 nm. Each operational parameter treatment is carried out three replications. The percentage of turquoise blue removal was determined using formula:

$$\text{Dye removal (\%)} = \frac{A_o - A_t}{A_o} \times 100\% \quad (1)$$

where: the A_o and A_t represents the dye absorbance at before and after treatment, respectively.

The initial pH solution effect

The impact of dye solution's initial pH on dye removal is investigated using the batch technique. As much as 100 mL of 25 mg/L blue-green dye was placed in the photocatalytic reactor, and the mixture was adjusted to an initial pH of 6. The dye solution in a reactor was added with 10.0 mg/L of AgNPs, and then it was irradiated with a 50-watt UV lamp for 180 mins. The same treatment was also carried out at different initial pH levels of turquoise blue dye, namely 4, 5, 7, 8, 9, and 10. A UV-visible spectrophotometer set at 615 nm was used to detect the dye absorbance before and after treatment.

The AgNPs to dye volume ratio effect

In this treatment, 10.0 mL of AgNPs was transferred to a reactor containing 100 mL of a turquoise blue dye solution at a concentration of 25 mg/L. The mixture in the reactor was adjusted to the ideal pH obtained by prior treatment and then irradiated with a 50-watt UV lamp for 180 minutes. Following treatment, Whatman No. 42 filter paper was used to filter the mixture, and a UV-visible spectrophotometer set at 615 nm was applied to detect the dye absorption. Using the same procedure, the dye treatment was carried out at various volumes of AgNPs addition, namely 2.0, 4.0, 6.0, and 8.0 mL per 100 mL of dye solution.

The dye concentration effect

As much as 100 mL of 25 mg/L turquoise blue textile dye was placed in a photocatalytic reactor, then AgNPs were added with the optimum volume of AgNPs as well as adjusted at the optimum pH obtained from the previous treatment. After 180 minutes of being irradiated with a 50-watt UV lamp, the mixture was filtered with

Whatman No. 42 filter paper. The dye absorbance before and after treatment was determined using a UV-visible spectrophotometer at a wavelength of 615 nm. The same process was also conducted at different concentrations of turquoise blue dye, including 50, 75, 100, 125, and 150 mg/L.

The irradiation duration time effect

To evaluate the UV light exposure time effect on the percentage of dye removal, a total volume of 100 mL turquoise blue textile dye was placed in a photocatalytic reactor and added with the optimum volume of AgNPs as well as adjusted at the optimum pH obtained from the previous treatment. The photocatalytic degradation process of dyes irradiated by 50-watt UV lamps was carried out at different UV lamp exposure times, namely 30, 60, 120, and 150 minutes. A UV-visible spectrophotometer set at 615 nm was applied to measure the dye absorbance both before and after treatment.

RESULTS AND DISCUSSIONS

Phytochemical screening of aqueous kecemcem leaf extract

A phytochemical screening test was aimed at identifying flavonoids, terpenoids, steroids, alkaloids, saponins, and tannins that act as bioreducers in the formation of AgNPs. The presence of these phytochemical compounds in Kecemcem leaf is conceded by the confirmatory test result, involving precipitate formation and changes in color. The qualitative phytochemical screening analysis results of Kecemcem leaf aqueous extract are summarised in Table 1.

Table 1 shows that the aqueous extract of Kecemcem leaf contains bioactive compounds of flavonoids, terpenoids, alkaloids, saponins, and tannins, while steroids were not found in this leaf extract. The existence of these bioactive substances is important for reduction of AgNO_3 in the synthesis of AgNPs. The Ag^+ ion can be reduced to Ag^0 by electron donation from flavonoid, terpenoid, alkaloid, saponin and tannin [Hemlata et al., 2015; Ahmed and Mustafa, 2020]. The development of a deep pink flavonoid precipitate using Shinod reagent indicated a positive flavonoid test [Komala, 2022]. Detection of the presence of alkaloids in the aqueous extract of Kecemcem leaf was carried out using Mayer, Wagner, and Dragendorff reagents. In Dragendorff's test,

Table 1. The identification result of phytochemical compound from Kecemcem leaf aqueous extract

Phytochemicals compound	Test/Reagents	Visual observation	Result
Flavonoid	Shinod's test HCl + Mg + extract → Deep pink color formed		Positive
Terpenoid	Liebermann-Buchard test Extract + acetic anhydride + H ₂ SO ₄ → Dark green color formed		Positive
Alkaloid	Dragendorff's test Dragendorff's reagent + extract. → Orange precipitate formed		Positive
	Wagner's test Wagner's reagent + extract → Brown reddish precipitate formed		Positive
	Mayer's test. Mayer's reagent + extract → Cream coloured precipitate formed		Positive
Steroids	Liebermann-Buchard test Extract + acetic anhydride + H ₂ SO ₄ → Green or blue color formation		Negative
Saponin	Na ₂ CO _{3(aq)} + extract → Foam formed		Positive
Tannin	Ferric chloride test → the dark blue formed		Positive

the formation of a red precipitate after the addition of potassium bismuth iodide to the aqueous extract of Kecemcem leaf indicates the presence of alkaloids. In Mayer's test, the formation of a yellowish colored precipitate after the addition of extract with a potassium mercuric iodide reagent indicates the presence of alkaloids. Meanwhile, in the Wagner test, the aqueous extract of Kecemcem leaf was added with a solution of iodine in potassium iodide and a reddish brown precipitate

was formed which indicated the presence of alkaloids [Pandey and Tripathi, 2014].

Characteristic of AgNPs

AgNPs absorption spectra in the UV-Vis

UV-visible spectroscopy is the most common method for confirming the creation of metallic nanoparticles. The main sign indicating the

formation of silver nanoparticles is when the mixture changes color from transparent to dark brown due to the reduction reaction of Ag^+ to Ag^0 [Jain et al., 2020]. The formation of AgNPs can be detected their UV-Vis absorbance spectrum in the scanning range of 300–800 nm as assigned in Figure 2.

As we can see in Figure 2, the UV-Visible spectrum obtains a maximum absorption band at 420 nm, which indicates the phytochemicals in the aqueous extract of Kecemcem leaf are effective in reducing Ag^+ ions to AgNPs because colloidal silver has a characteristic absorption band in the range of 400–450 nm [Gopalakrishnan et al., 2023]. In aqueous solution, AgNPs were dark brown in color due to electron excitation and changes in electronic energy levels, which indicated the reduction of Ag^+ to Ag^0 [Elemike et al., 2017]. The same absorption band at 420 nm was also observed for silver nanoparticles synthesized using *Streptomyces* sp. [Karthik et al., 2014].

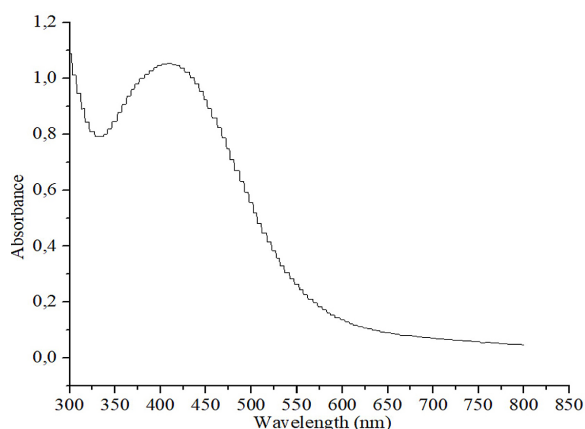


Figure 2. UV-Vis spectrum of AgNPs synthesized using Kecemcem leaf aqueous extract

However, several research results found a strong peak from UV-Visible spectroscopy of AgNPs synthesized using *Thunbergia grandiflora* leaf extract appearing at 441 nm [Varadavenkatesan et al., 2024], and AgNPs synthesized using *Calendula officinalis* leaves were observed at 436 nm [Paul et al., 2020].

FTIR analysis

The FTIR spectrophotometer is applied to identify the major functional groups associated with the AgNPs and the phytochemicals, such as the flavonoids, terpenoids, alkaloids, steroids, saponins, and tannins obtained in an aqueous extract of Kecemcem leaf. The FTIR spectrum of phytochemical compounds from the aqueous extract of Kecemcem leaf recorded in the region of wavenumbers 500–4000 cm^{-1} is presented in Figure 3.

The FTIR absorption band of the Kecemcem leaf aqueous extract appeared at 3651.25 cm^{-1} , 2985.51 cm^{-1} , 2303.79 cm^{-1} , 1,695.43 cm^{-1} , and 817.82 cm^{-1} , respectively. The band observed at 3651.25 cm^{-1} can be associated to the hydroxyl group (OH) functional group. The signal appearing around the wave number 2985.81 cm^{-1} may be caused by the C-H stretching of the methylene group or aliphatic group, and this also confirms the presence of saponins in the aqueous extract of Kecemcem leaf. The FTIR signal that appears at 1695.43 cm^{-1} can be associated to the C=C function of terpenoids. This is reinforced by the fact that terpenoids often show absorption bands in the 1450–1700 cm^{-1} region due to the presence of C=C bonds [Malik et al., 2018]. Furthermore, the reduction of Ag^+ to form Ag^0 by bioreductor contain in Kecemcem leaf aqueous extract, makes

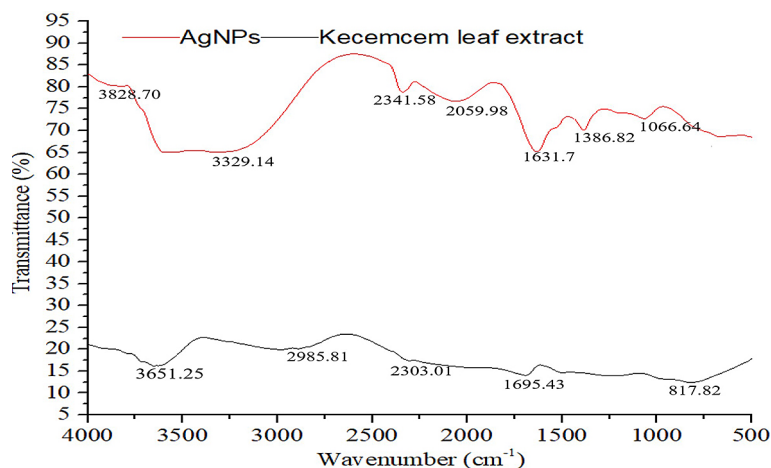


Figure 3. FTIR spectrum for aqueous extract of Kecemcem leaf and AgNPs

the peaks are shifted to a higher wavenumber such as 3828.70 cm^{-1} , 3329.14 cm^{-1} , 2341.58 cm^{-1} , 2059.98 cm^{-1} , and 1066.64 cm^{-1} , respectively. As we seen in Figure 3, the FTIR spectrum of synthesized AgNPs peaks at 3329.14 cm^{-1} may be attributed to OH stretching. Similarly, the IR spectrum peaks at 1631.7 cm^{-1} and 1386.62 cm^{-1} attributed to the C=C stretching of cyclic alkene and C-H stretching of amide bond confirmed the presence of protein [Al-Nuairi et al., 2020]. Peak observed at 1066.64 cm^{-1} coresspond to C-O stretching of carbonyl functional group [Nouri et al., 2020].

XRD analysis

XRD spectrophotometer were applied to identify the crystalline phase, structure and size of AgNPs synthesized from Kecemcem leaf extract. The XRD pattern analysis of synthesized AgNPs using aqueous extract of Kecemcem leaf is presented in Figure 4.

Figure 3 shows the XRD pattern of AgNPs, which has five diffraction peaks at 2θ values of 31.60° , 38.45° , 43.97° , 64.01° , and 77.62° . Examination of the crystallinity degree of AgNPs based on the XRD pattern using Origin version 8.5.1, and was found to be 54.35% with average size of crystalline was 22 nm. According to Trieu et al.(2023), the diffraction pattern related to Ag metal was exhibited at 2θ values 38.3° , 44.1° , 64.6° , and 77.5° which are considered with (111), (200), (220), and (311) respectively planes, confirm to cubic face-centered structure. In addition, studies conducted by Riaz et al. (2020) and Githala et al. (2022) also confirmed that the X-ray diffraction patterns of AgNPs at 2θ around 38.22° , 46.32° , 64.34° , and 76.46° were associated with

the (111), (200), (220), and (311) planes, respectively confirm the cubic face-centered structure.

Photocatalytic degradation studies

The photocatalytic degradation of turquoise blue dye in aqueous solution was done using synthesized AgNPs as a catalyst. The catalyst was irradiated with 50 watts of UV lamp. The operating conditional were investigate involving the effect of pH, dye concentration, volume addition of AgNPs and exposure duration time.

The initial pH effect

The pH is one of a crucial operating parameter factors in the degradation activity of AgNPs, because the pH affect the surface charge of AgNPs and dissociation ability of turquoise blue dye. In acidic media, more H^+ ions can be accessed on the surface of AgNPs, causing the surface to become more positively charged, thus increasing the photocatalytic activity due to the strong interaction between AgNPs and the anionic turquoise blue dye. However, in alkaline conditions, the strong force of repulsion between the negative charge AgNPs surface and the anionic turquoise blue dye makes it difficult for anionic dye molecules to get adsorbed on the surface of AgNPs. Therefore, this repulsion contributes to decreasing the photocatalytic degradation efficiency under basic conditions [Khan et al., 2024]. The optimum environment's pH level required for photocatalytic degradation process of dyes varies depending on the specific photocatalyst and the dye types. To investigate the optimum pH in dye removal, 100 mL of turquoise blue dye with a concentration of

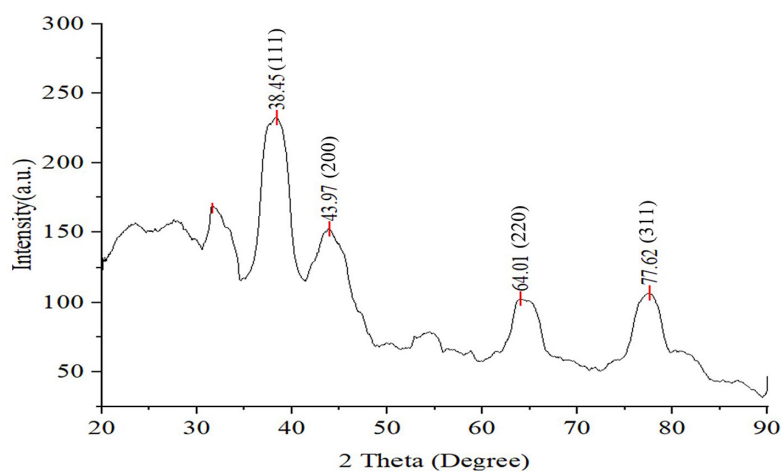


Figure 4. XRD pattern for AgNPs

25 mg/L were treated for 180 min. with a 10.0 mL AgNPs suspension at different pHs of 4–10. The removal photocatalytic efficiency of AgNPs against turquoise blue dye removal in different pH mediums is presented in Figure 5.

Figure 5 shows the removal photocatalytic efficiency slightly increased from 9.02% to 90.26% when the pH increased from 4 to 5 and then the efficiency decreased gradually up to pH of 10. The AgNPs photocatalytic activity against blue-green textile dye in a solution irradiated with 50 watts of UV light for 180 minutes, which was optimal at pH 5 with a removal efficiency of 90.26%. Similar findings have been observed by other researchers such as Devi and Dhurai, (2023) who report the highest color removal photocatalytic efficiency of anionic *colomill brilliant red 3BN* acid dye by AgNPs synthesized using *Pongamia pinnata* leaf extract was obtained at pH 4. However, Bassim et al. (2023) who found that the photocatalytic degradation efficiency of CuO/TiO₂ nanoparticles synthesized using citrus aurantium fruit extract against cationic methylene blue dye at pH 3 was 46.3% and increased drastically to 92.6% at pH 9. In acidic conditions, the AgNPs surfaces have a negative charge, and the turquoise blue dye is an anionic dye type. As a consequence, mighty adhesion between AgNPs and this dye leads to increased photocatalytic activity. In addition, the pH point zero charge (PZC) of AgNP greatly affects the strength of its interaction with the dye, which directly impacts the photocatalytic activity. The PZC refers to the specific pH at which the net charge of the AgNPs is neutralized, resulting in a total charge of zero. As reported in some literatures, the PZC of AgNPs

is about 8.5, which implies that at pH values lower than 8.5, the surface of AgNPs will predominantly have positive charges, while at pH above 8.6, they tend to have negative charges [Ezeuko et al., 2022; Castellar-Ortega, et al., 2022; Singh et al., 2023].

The AgNPs-to-dye volume ratio effect

The effect of the AgNPs-to-dye ratio on the photocatalytic degradation ability against turquoise blue dye was examined using variations in the volume of AgNPs colloidal suspension (2, 4, 6, 8, and 10 mL) against a fixed volume of 100 mL of dye with a concentration of 25 mg/L. The removal efficiency of turquoise blue dye using various volume of AgNPs is presented in Figure 6.

As seen in Figure 6, Increasing the volume of AgNPs colloidal suspension used for the photocatalytic degradation process will generate the electron-hole pairs or increase the formation of radical hydroxyl ($\bullet\text{OH}$) and thus cause a faster turquoise blue dye degradation process. In this study, the treatment of 100 mL of 25 mg/L turquoise blue textile dye for 180 minutes using varying volumes of AgNPs (2, 4, 6, 8, and 10 mL) irradiated with 50 watts of UV light provided degradation efficiencies of 61.49%, 77.96%, 89.79%, 90.23%, and 90.26%, respectively. The photocatalytic activity increased drastically starting from the addition of 2 mL to 6 mL of AgNPs, then their activity increased slightly after the addition of the AgNPs volume from 8 mL to 10 mL. Similar findings were also reported by Hosseini-Zori and Shourijeh (2018), that photocatalytic activity increased in line with the increase in the concentration of photocatalyst used, but photocatalytic activity

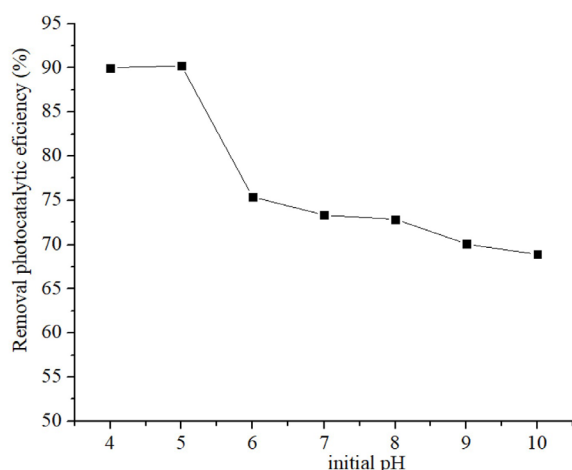


Figure 5. The photocatalytic degradation of turquoise blue dye using AgNPs at different initial pH medium

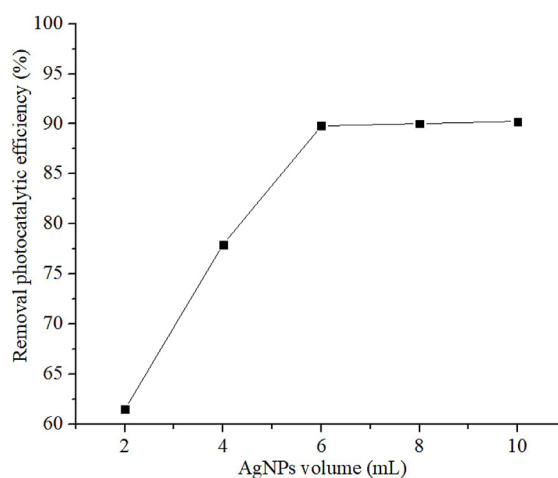


Figure 6. The photocatalytic degradation of turquoise blue dye at different AgNPs-to-dye volume ratios

decreased after further increase in the amount of photocatalyst. The decrease in photocatalytic activity at higher doses of AgNPs is associated with an increase in the turbidity of the liquid medium, which tends to scatter light, thus reducing its photocatalytic activity [Khan et al., 2024].

The initial dye concentration effect

Dye concentration influences the light penetration during the photocatalysis process. In this treatment, the AgNPs synthesized photocatalytic activity against turquoise blue dye in different dye concentration at range of 25–150 mg/L was assessed, and its result is depicted in Figure 7.

Figure 7 provides a visual depiction of the degradation efficiency of turquoise blue dye over a fixed duration of 180 minutes. As seen in Figure 7, the photocatalytic degradation efficiency increased with increasing dye concentration from 25 mg/L to 100 mg/L, then it decreased slightly at a dye concentration of 125 mg/L, while there was a drastic decrease at a dye concentration of 150 mg/L. The decrease in photocatalytic degradation efficiency in high dye concentration treatment may be associated with the inhibition of photon absorption on the AgNPs surface [Wang et al., 2022]. According to Bopape et al. (2024), a decrease in the quantity of photons that reach the photocatalyst surface is influenced by the increasing number of dye molecules that are absorbed on the surface. In this research, the maximum concentration of dye solution that can be treated to produce optimum degradation efficiency is 125 mg/L with a degradation percentage of 94.35%. This finding consistent with Alshehri et al. (2019), who studied the photocatalytic degradation process of MB at various concentrations in the range of 2.0×10^{-5} to 12×10^{-5} M. The results of their study showed that the removal efficiency reduced with increasing concentration of MB dye, where the optimal dye dose was obtained at 1×10^{-5} M.

The exposure duration time effect

The exposure duration time effect on the activity of turquoise blue dye photocatalytic degradation using AgNPs was investigated at pH 5.0, applying 100 mL of dye with a concentration of 125 mg/L and 6 mL of AgNPs colloidal suspension irradiated with a 50-watt UV lamp for 30–180 min. of duration time. The removal photocatalytic degradation efficiency of turquoise blue dye using AgNPs at different exposure duration times

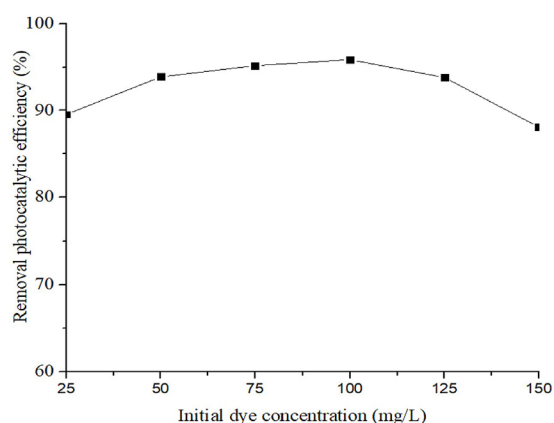


Figure 7. The photocatalytic degradation of turquoise blue using AgNPs at different initial dye concentration

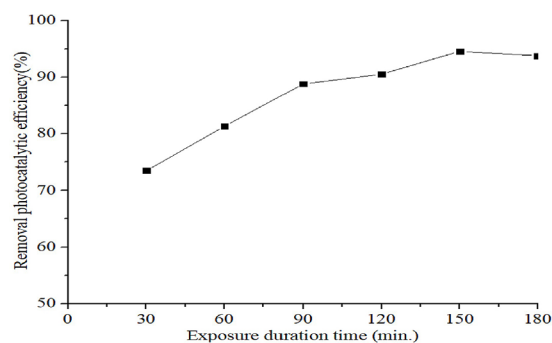


Figure 8. The photocatalytic degradation of turquoise blue using AgNPs at different exposure duration time

was assigned in Figure 8. Figure 8 clearly shows that the photocatalytic activity rate increases rapidly at exposure duration up to 90 min, and then the photocatalytic activity slows down at contact time from 90 to 150 min and finally decreases at contact time from 150 to 180 min. The photocatalytic degradation efficiency in successive of 73.45%, 81.32%, 88.80%, 90.52%, 94.57%, and 93.79% was observed after 30, 60, 90, 120, 150, and 180 mins. of exposure time. This finding is in line with Parethe et al. (2024), who reported that the photocatalytic degradation of methylene blue is a function of contact time between the dye and cobalt oxide nanoparticles, where the degradation efficiency increased with increasing contact time.

CONCLUSIONS

This study focused on degrading turquoise blue textile dyes photocatalytically using silver nanoparticles irradiated by UV light. The results

of this research were that silver nanoparticles prepared using a reductant from Kecemcem leaf extract were able to degrade turquoise blue anionic dyes effectively and efficiently. The percentage of photocatalytic degradation of 100 mL of turquoise blue textile dyes with a concentration of 125 mg/L was obtained at 94.57% in 150 minutes of exposure time, with operating parameters including pH 5, UV lamp intensity of 50 watts, and the volume of AgNPs used was 6 mL per 100 mL of dye solution. With high degradation efficiency, silver nanoparticles synthesized with Kecemcem leaf extract have great potential to be applied in the removal textile wastewater.

Acknowledgments

The author would like to express his gratitude to the Doctoral Program in Environmental Science, Udayana University for providing facilities to conduct this research.

REFERENCES

- Abada, E., Mashraqi, A., Modafar, Y., Al-Abboud, M.A., & El-Shabasy, E. (2024). Review green synthesis of silver nanoparticles by using plant extracts and their antimicrobial activity. *Saudi Journal of Biological Sciences*, 31(1), 103877. <https://doi.org/10.1016/j.sjbs.2023.103877>
- Ahmed, R.H., & Mustafa, D.E. (2020). Green Synthesis of Silver nanoparticles mediated by traditionally used medicinal plants in Sudan. *International Nano Letters*, 10, 1–14. <https://doi.org/10.1007/s40089-019-00291-9>
- Alshehri, A.A., & Malik M.A. (2019). Biogenic fabrication of ZnO nanoparticles using *Trigonella foenum-graecum* (Fenugreek) for proficient photocatalytic degradation of methylene blue under UV irradiation. *Materials in Electronics*, 30, 16156–16173. <https://doi.org/10.1007/s10854-019-01985-8>
- Al-Nuairi, A.G., Mosa, K.A., Mohammad, M.G., El-Keblawy, A., Soliman, S., & Alawadhi, H. (2020). Biosynthesis, characterization, and evaluation of the cytotoxic effects of biologically synthesized silver nanoparticles from cyperus conglomeratus root extracts on breast cancer cell line MCF-7. *Biological Trace Element Research*, 194(2), 560–569. <https://doi.org/10.1007/s12011-019-01791-7>
- Bassim, S., Mageed, A.K., AbdulRazak, A.A., & Al-Sheikh, F. (2023). Photodegradation of methylene blue with aid of green synthesis of CuO/TiO₂ nanoparticles from extract of citrus aurantium juice. *Bulletin of Chemical Reaction Engineering & Catalysis*, 18(1), 1–16. <https://doi.org/10.9767/bcrec.16417>
- Bopape, D.A., Ntsendwana, B., & Mabasa, F.D. (2024). Photocatalysis as a pre-discharge treatment to improve the effect of textile dyes on human health: A critical review. *Heliyon*, 10(20), e39316. <https://doi.org/10.1016/j.heliyon.2024.e39316>
- Bressan, L.G., Flores, G.C.P., Biolchi, N.J., Mendes, M.E.S., Dervanoski, A., Korf, E.P., & Pasquali, G.D.L. (2024). Comparison of electrocoagulation and physicochemical coagulation/flocculation in the treatment of synthetic textile wastewater. *Brazilian Journal of Environmental Sciences*, v.59, e18803. <https://doi.org/10.5327/Z2176-94781803>
- Cahyawati, P.N., Lestari, A., Subrata, T., Dewi, N.W.E.S., Wiadnyana, I.G.P. (2019). Phytochemical test on herbal drinks loloh Cemcem at Penglipuran Village, Bali. *Journal of Physics: Conference Series*, 1402, 055030.
- Castellar-Ortega, G.C., Cely-Bautista, M.M., Cardozo-Arrieta, B.M., Jaramillo-Colpas, J.E., Moreno-Aldana, L.C., & Valencia-Ríos, J.S. (2022). Evaluation of diatomaceous earth in the removal of crystal violet dye in solution. *Journal of applied research and technology*, 20(4), 387–398. <https://doi.org/10.22201/icat.24486736e.2022.20.4.1524>
- Devi, R.S., & Dhurai, B. (2023). Synthesis of silver nanoparticles using Pongamia pinnata leaf extract for efficient removal of acid brilliant red 3BN dye under solar irradiation. *Desalination and Water Treatment*, 315, 373–386. <https://doi.org/10.5004/dwt.2023.30149>
- Dhameliya, K.B., & Ambasana, C. (2023). Assessment of wastewater contaminants caused by textile industries. *Journal of Pure and Applied Microbiology*, 17(3), 1477–1485. <https://doi.org/10.22207/JPAM.17.3.09>
- Elemike, E.E., Onwudiwe, D.C., & Arijeh, O. (2017). Plant-mediated biosynthesis of silver nanoparticles by leaf extracts of *Lasienthra africanum* and a study of the influence of kinetic parameters. *Bulletin of Materials Science*, 40, 129–137. <https://doi.org/10.1007/s12034-017-1362-8>
- El-Sayed, E., El-Aziz, E.A., Othman H.A., & Hassabo A.G. (2024). Azo dyes: Synthesis, classification and utilisation in textile industry. *Egyptian Journal of Chemistry*, 67, 87–97. <https://doi.org/10.21608/ejchem.2024.257952.9057>
- Ezeuko, A., Ojemayo, M.O., Okoh, O.O., & Okoh, A.I. (2022). The effectiveness of silver nanoparticles as a clean-up material for water polluted with bacteria DNA conveying antibiotics resistance genes: Effect of different molar concentrations and competing ions. *OpenNano*, 7, 1000060. <https://doi.org/10.1016/j.onano.2022.1000060>
- Fajri, J.A., Nurmiyanto, A., Sa'adah, N.N., Nuryana, I.N., Anfaresi, S.L.N., & Lathifah, A.N. (2024).

- Effectiveness of endophytes bacteria in enhancing floating treatment wetland to treat textile wastewater. *Journal of Ecological Engineering*, 25(3), 12–24. <https://doi.org/10.12911/22998993/177593>
16. Garciduenas-Pina, C., Tirado-Fuentes, C., Ruiz-Peréz, J., Valerio-García, R.C., & Morales-Domínguez, J.F. (2023). Silver nanoparticles synthesized with extracts of leaves of *Raphanus sativus* L., *Beta vulgaris* L., and *Ocimum basilicum* and Its Application in seed disinfection. *Nanomaterials and Nanotechnology*, 2023, 874979. <https://doi.org/10.1155/2023/9874979>
 17. Githala, C.K., Raj, S., Dhaka, A., Mali, S.C., & Trivedi, R. (2022). Phyto-fabrication of silver nanoparticles and their catalytic dye degradation and antifungal efficacy. *Frontiers in Chemistry*, 10, 994721. <https://doi.org/10.3389/fchem.2022.994721>
 18. Gopalakrishnan, K., Chandel, M., Gupta, V., Kaur, Kuljinder, Patel, A., Kaur, Kamaljit, Kishore A., Prabhakar, P.K., Singh, A., Shankar, Prasad, J., Bodana, V., Saxena, V., Shanmugam, V., & Sharma, A. (2023). Valorisation of fruit peel bioactive into green synthesized silver nanoparticles to modify cellulose wrapper for shelf-life extension of packaged bread. *Food Research International*, 164, 112321. <https://doi.org/10.1016/j.foodres.2022.112321>
 19. Hemlata, Mena, P.R., Singh, A.P., & Tejavath, K.K. (2015). Biosynthesis of Silver nanoparticles using cucumis prophetarum aqueous leaf extract and their antibacterial and antiproliferative activity against cancer cell lines. *ACS Omega*, 5(10), 5520–5528.
 20. Hosseini-Zori, M., & Shourijeh, Z.M. (2018). Synthesis, Characterization and investigation of photocatalytic activity of transition metal-doped TiO₂ nanostructures. *Progress in Color, Colorants and Coatings*, 1(4), 209–220. <https://doi.org/10.30509/pccc.2018.76671>
 21. Jaast, S., & Grewal, A. (2021). Green synthesis of silver nanoparticles, characterization and evaluation of their photocatalytic dye degradation activity. *Current Research in Green and Sustainability Chemistry*, 4, 100195. <https://doi.org/10.1016/j.crgsc.2021.100195>
 22. Jain, A., Ahmad, F., Gola, D., Malik, A., Chauhan, N., Dey, P., & Tyagi, P. K. (2020). Multi dye degradation and antibacterial potential of papaya leaf derived silver nanoparticles. *Environmental Nanotechnology, Monitoring and Management*, 14, 100337. <https://doi.org/10.1016/j.enmm.2020.100337>
 23. Karthik, L., Kumar, G., & Bhaskara Rao, K.V. (2014). Streptomyces sp. LK3 mediated synthesis of silver nanoparticles and its biomedical application. *Bioprocess and Biosystems Engineering*, 37, 261–267. <https://doi.org/10.1007/s00449-013-0994-3>
 24. Khan, S., Noor, T., Iqbal, N., & Yaqoob, L. (2024). Photocatalytic dye degradation from textile wastewater: A review. *ACS Omega*, 9(20), 21751–21767. <https://doi.org/10.1021/acsomega.4c00887>
 25. Khan, S., Zahoor, M., Khan, R.S., Ikram, M., & Islam, N.U. (2023). The impact of silver nanoparticles on the growth of plants: The agriculture applications. *Heliyon*, 9(6), e16928. <https://doi.org/10.1016/j.heliyon.2023.e16928>
 26. Komala, V.V.D.M. (2022). Qualitative, quantitative phytochemical analysis and in-vitro anti-mycobacterial evaluation of allspice. *International Journal of Health Sciences*, 6(S6), 2564–2581. <https://doi.org/10.53730/ijhs.v6nS6.9868>
 27. Kumar, U. (2017). Performance evaluation of effluent treatment plant of SRF limited, malanpur blind. *International Journal for Research in Applied Science and Engineering Technology*, 5(4), 1475–1478.
 28. Malik, S.K., Ahmed, M., & Khan, F. (2018). Identification of novel anticancer terpenoids from *Prosopis juliflora* (Sw) DC (Leguminosae) pods. *Tropical Journal of Pharmaceutical Research*, 17(4), 661–668. <http://dx.doi.org/10.4314/tjpr.v17i4.14>
 29. Meher, A., Tandi, A., Moharana, S., Chakraborty, S., Mohapatra, S.S., Mondal, A., Dey, S., & Chandra, P. (2024). Silver nanoparticle for biomedical applications: A review. *Hybrid Advances*, 6, 100184. <https://doi.org/10.1016/j.hybadv.2024.100184>
 30. Nazri, M.K.H.M., & Sapawe, N. (2020). A short review on photocatalytic toward dye degradation. *Materialstoday Proceedings*. 31(1), A42–A47. <https://doi.org/10.1016/j.matpr.2020.10.967>
 31. Nouri, A., Yarak, M.T., Lajevardi, A., Rezaei, Z., Ghorbanpour, M., & Tanzifi, M. (2020). Ultrasonic-assisted green synthesis of silver nanoparticles using *Mentha aquatica* leaf extract for enhanced antibacterial properties and catalytic activity. *Colloid and Interface Science Communications*, 35, 100252. <https://doi.org/10.1016/j.colcom.2020.100252>
 32. Pandey, A., & Tripathi, S. (2014). Concept of standardization, extraction and pre phytochemical screening strategies for herbal drug, *Journal of Pharmacognosy and Phytochemistry*. 2(5), 115–119.
 33. Parvathiraja, C., Shailajha, S., Shanavas, S., & Guring, J. (2021). Biosynthesis of silver nanoparticles by *Cyperus pangorei* and its potential in structural, optical and catalytic dye degradation. *Applied Nanoscience*, 11, 477–491. <https://doi.org/10.1007/s13204-020-01585-7>
 34. Parethe, G.T., Rajesh, P., Velmani, V., Balaji, M., & Kavica, S. (2024). Enhanced Photocatalytic Degradation of methylene blue dye using Co₃O₄ nanoparticles from the fruit extracts of *diplocyclos Palmatus* (L) C. Jeffrey for wastewater remediation. *Journal of Water and Environmental Nanotechnology*, 9(3), 356–366.
 35. Paul, S.C., Bhowmik, S., Nath, M.R., Islam, M.D.S., Paul, S.K., Neaz, J., Monir, T.S.B., Dewanjee, S., & Salam, M.A. (2020). Silver nanoparticles synthesis in a green approach: Size dependent catalytic degradation of cationic and anionic dyes. *Oriental*

- Journal of Chemistry*. 36(3), 353–360.
36. Pingmuang, K., Chen, J., Kangwansupamonkon, W., Wallace, G.G., Phanichphant, S., & Nattestad, A. (2017). Composite photocatalysts containing BiVO₄ for degradation of cationic dyes. *Scientific Reports*, 7. <https://doi.org/10.1038/s41598-017-09514-5>
 37. Riaz, M., Ismail, M., Ahmad, B., Zahid, Z., Jabbour, G., Khan, M.S., Mutreja, V., Sareen, S., Rafiq, A., Faheem, M., Shah, M.M., Khan, M.I., Bukhari, S.A.I., & Park, J. (2020). Characterizations and analysis of the antioxidant, antimicrobial, and dye reduction ability of green synthesized silver nanoparticles. *Green Processing and Synthesis*, 9, 693–705. <https://doi.org/10.1515/gps-2020-0064>
 38. Saeed, M., Muneer, M., ul-Haq, A., & Akram, N. (2022). Photocatalysis: an effective tool for photodegradation of dyes: a review. *Environmental Science and Pollution Research*, 29, 293–311. <https://doi.org/10.1007/s11356-021-16389-7>
 39. Salve, M., Mandal, A., Amreen, K., Pattnaik, P.K., & Goel, S. (2020). Greenly synthesized silver nanoparticles for supercapacitor and electrochemical sensing applications in a 3D printed microfluidic platform. *Microchemical Journal*, 157, 104973. <https://doi.org/10.1016/j.microc.2020.104973>
 40. Singh, V., Pant, N., Sharma, R.K., Padalia, D., Rawat, P.S., Goswami, R., & Deifalla, A.M. (2023). Adsorption studies of Pb (II) and Cd (II) heavy metal ions from aqueous solutions using a magnetic biochar composite material. *Separations*, 10(7), 389. <https://doi.org/10.3390/separations10070389>
 41. Strebel, A., Behringer, M., Hilbig, H., Machner, A., & Helmreich, B. (2024). Anionic azo dyes and their removal from textile wastewater through adsorption by various adsorbents: a critical review. *Frontiers in Environmental Engineering*, 3, 1–17. <https://doi.org/10.3389/fenv.2024.1347981>
 42. Suidiana, I.K., Sastrawidana, I.D.K., & Sukarta, I.N. (2022). Adsorption kinetic and isotherm studies of reactive red B textile dye removal using activated coconut leaf stalk. *Ecological Engineering & Environmental Technology*, 23(5), 61–71. <https://doi.org/10.12912/27197050/151628>
 43. Suidiana, I.K., Citrawathi, D.M., Sastrawidana, I.D.K., Maryam, S., Sukarta, I.N., & Wirawan, G.A.H. (2022). Biodegradation of turquoise blue textile dye by wood degrading local fungi Isolated from plantation area. *Journal of Ecological Engineering*, 23(7), 205–214. <https://doi.org/10.12911/22998993/150044>
 44. Sujarwo, W., Keim, A.P., Savo V., Guarrera, P.M., & Caneva G. (2015). Ethnobotanical study of Loloh: Traditional herbal drinks from Bali (Indonesia). *Journal of Ethnopharmacol*, 1(169), 34–48. <https://doi.org/10.1016/j.jep.2015.03.079>
 45. Sukarta, I.N., & Sastrawidana, I.D.K. (2024). Synthesis and characterization of hydroxyapatite/titania composite and its application on photocatalytic degradation of remazol red B textile dye under UV irradiation. *Ecological Engineering and Environmental Technology*. 25(2), 178–189. <https://doi.org/10.12912/27197050/176230>
 46. Sukarta, I.N., Ayuni, N.P.S., & Sastrawidana, I.D.K. (2021). Utilization of khamir (*Saccharomyces cerevisiae*) as adsorbent of remazol red RB textile dyes. *Ecological Engineering & Environmental Technology*. 22(1), 117–123. <https://doi.org/10.12912/27197050/132087>
 47. Tabish, M., Tabinda, A.B., Mazhar, Z., Yasar, A., Ansar, J., & Wasif, I. (2024). Physical, chemical and biological treatment of textile wastewater for removal of dyes and heavy metals. *Desalination and Water Treatment*, 320, 100842 <https://doi.org/10.1016/j.dwt.2024.100842>
 48. Trieu, Q.A., Le, C.T.B., Pham, C.M., & Huu, T. (2023). Photocatalytic degradation of methylene blue and antibacterial activity of silver nanoparticles synthesized from *Camellia sinensis* leaf extract. *Journal of Experimental Nanoscience*, 18(1), 2225759. <https://doi.org/10.1080/17458080.2023.2225759>
 49. Varadavenkatesan, T., Nagendran, V., Vimayagam, R., Goveas, L.C., & Selvaraj, R. (2024). Effective degradation of dyes using silver nanoparticles synthesized from *Thunbergia grandiflora* leaf extract. *Bioresource Technology Reports*, 27, 101914. <https://doi.org/10.1016/j.biteb.2024.101914>
 50. Velusamy, P., Das J., Pachaiappan, R., Vaseeharan, B., & Pandian, K. (2015). Greener approach for synthesis of antibacterial silver nanoparticles using aqueous solution of neem gum (*Azadirachta indica* L.). *Industrial Crops and Products*, 66, 103–109. <https://doi.org/10.1016/j.indcrop.2014.12.042>
 51. Verma, A., & Mehata, M.S. (2016). Controllable synthesis of silver nanoparticles using neem leaves and their antimicrobial activity. *Journal of Radiation Research and Applied Sciences*, 9(1), 109–115. <https://doi.org/10.1016/j.jrras.2015.11.001>
 52. Wang, L., Liu, S., Li, J., & Li S. (2022). Effects of several organic fertilizers on heavy metal passivation in Cd-contaminated gray-purple soil. *Frontiers in Environmental Science*, 10, 895646. <https://doi.org/10.3389/fenvs.2022.895646>
 53. Xu, L., Wang, Y.Y., Huang, J., Chen, C.Y., Wang, Z.X., & Xie, H. (2020). Silver nanoparticles: Synthesis, medical applications and biosafety. *Theranostics*, 10(20), 8996–9031. <https://doi.org/10.7150/thno.45413>
 54. Zayed, M.A., Abo-Ayad, Z.A., & Medany, S.S. (2021). Catalytic efficient electro-oxidation degradation of DO26 textile dye via UV/VIS, COD, and GC/MS evaluation of byproducts. *Electrocatalysis*, 12(6), 731–746. <https://doi.org/10.1007/s12678-021-00683-6>